

# PCCP

Accepted Manuscript



This is an *Accepted Manuscript*, which has been through the Royal Society of Chemistry peer review process and has been accepted for publication.

*Accepted Manuscripts* are published online shortly after acceptance, before technical editing, formatting and proof reading. Using this free service, authors can make their results available to the community, in citable form, before we publish the edited article. We will replace this *Accepted Manuscript* with the edited and formatted *Advance Article* as soon as it is available.

You can find more information about *Accepted Manuscripts* in the [Information for Authors](#).

Please note that technical editing may introduce minor changes to the text and/or graphics, which may alter content. The journal's standard [Terms & Conditions](#) and the [Ethical guidelines](#) still apply. In no event shall the Royal Society of Chemistry be held responsible for any errors or omissions in this *Accepted Manuscript* or any consequences arising from the use of any information it contains.

1     **EXPLORING THE CHARGED NATURE OF SUPRAMOLECULAR MICELLES BASED ON P-**  
2     **SULFONATOCALIX[6]ARENE AND DODECYLTRIMETHYLAMMONIUM BROMIDE**

3

4     Nuno Basílio<sup>\*a</sup>, Daniel Alfonso Spudeit<sup>b</sup>, Juliana Bastos<sup>b</sup>, Leandro Scorsin<sup>b</sup>, Haidi D. Fiedler<sup>b</sup>,  
5     Faruk Nome<sup>b</sup>, Luis García-Río<sup>\*c</sup>

6

7     <sup>a</sup>Laboratório Associado para a Química Verde (LAQV), REQUIMTE, Departamento de Química,  
8     Faculdade de Ciências e Tecnologia, Universidade Nova de Lisboa, 2829-516 Monte de  
9     Caparica, Portugal.

10    <sup>b</sup>INCT-Catálise, Departamento de Química, Universidade Federal de Santa Catarina, 88040-  
11    900Florianópolis, Santa Catarina, Brazil.

12    <sup>c</sup>Departamento de QuímicaFísica, Centro de Investigación en Química Biológica y Materiales  
13    Moleculares (CIQUS), Universidad de Santiago de Compostela, 15782 Santiago de Compostela,  
14    Spain.

15

16

17

18

19

20 **ABSTRACT**

21 The aggregation of supramolecular amphiphiles formed from hexamethylated *p*-  
22 sulfonatocalix[6]arene (SC6HM) and dodecyltrimethylammonium bromide (C<sub>12</sub>TAB) was  
23 studied by capillary electrophoresis experiments and by kinetic probes. The hydrolysis of 4-  
24 methoxybenzenesulfonyl chloride (MBSC) was used to investigate the micropolarity of the  
25 micellar aggregates and their ability to solubilize and stabilize labile organic compounds against  
26 hydrolysis. Further insights were obtained using a more sophisticated kinetic probe: the basic  
27 hydrolysis of *p*-nitrophenylvalerate (NPV). This probe provides information on the ionic  
28 composition of the micellar interface and on the potential of the aggregates to be used as  
29 nanoreactors. The results obtained revealed that the charge of the micellar aggregates can be tuned  
30 from anionic to cationic through the adjustment of the C<sub>12</sub>TAB:SC6HM molar ratio and  
31 confirmed that these micelles have good solubilization properties. On the other hand, the  
32 kinetics of the *p*-nitrophenylvalerate basic hydrolysis suggest that, in the concentration range  
33 comprised between the first and second CMC's, Br<sup>-</sup> anions do not take part of the micellar  
34 structure.

35

36

37 **INTRODUCTION**

38 Surfactants are amphiphiles, molecules that contain hydrophobic and hydrophilic segments.<sup>1,2</sup>  
39 Compounds of this sort are ubiquitous in biological systems, as main components of membranes  
40 bilayers, and also find use in numerous technological and industrial applications: from common  
41 cleaning detergents to oil recovery, pharmaceutical and cosmetic formulations, drug delivery  
42 systems, catalysis and synthesis of nanostructured advanced materials, to name a few. All of  
43 these applications arise from the ability of these molecules to adsorb at surfaces and interfaces  
44 and to self-assemble into more or less defined aggregates of nanometric dimensions.

45 Conventional surfactants consist of a polar or ionic head group connected to a  
46 hydrophobic alkyl chain. Despite of their relative structural simplicity when dissolved in water  
47 these compounds can become involved in complex equilibria between free monomers,  
48 interfacial adsorption and aggregation. These phenomena have been the subject of numerous  
49 studies, but are not yet fully understood.<sup>3-5</sup> In addition to conventional surfactants, in recent  
50 years a new class of amphiphilic compounds emerged, the so-called supramolecular  
51 amphiphiles. The main difference between conventional and supramolecular amphiphiles is that  
52 in the former case the hydrophilic and hydrophobic segments are connected via covalent bonds,  
53 while in the latter case these segments are hold together by non-covalent interactions or  
54 dynamic covalent bonds.<sup>6-8</sup> While, as discussed above, the adsorption and aggregation  
55 properties of conventional surfactants are not fully understood, the field of supra-amphiphiles is  
56 in its infancy and the physico-chemical basis for the aggregation behavior of this special class of  
57 amphiphilic compounds is yet to be established.

58 The aggregation of supramolecular amphiphiles based on water soluble *p*-  
59 sulfonatocalix[n]arenes and cationic organic guests has attracted the attention of some research  
60 groups during the last years.<sup>9-26</sup> The stability and final architecture of the self-assembled  
61 aggregate depend strongly on the concentration ratio and structural features of both guest and  
62 host. For example, highly flexible *p*-sulfonatocalix[n]arenes methylated at the lower rim form  
63 micelle-like aggregates in the presence of cationic surfactants while native *p*-  
64 sulfonatocalix[n]arenes, which are conformationally less mobile due to intramolecular hydrogen

65 bonding between the hydroxyl groups, self-assemble into unilamellar vesicles and multilamellar  
66 nanoparticles in the presence of positively charged amphiphiles.<sup>9-26</sup>

67 The micellar aggregation of hexamethylated *p*-sulfonatocalix[6]arene (SC6HM) in the  
68 presence of cationic surfactants displays very interesting behavior and shares some features with  
69 oppositely charged polyelectrolyte/surfactant systems that deserve to be investigated in  
70 detail.<sup>9,12,13</sup> The critical micelle concentration ( $CMC_0$ ) of pure dodecyltrimethylammonium  
71 bromide ( $C_{12}TAB$ ) is  $CMC_0=14$  mM and in the presence of SC6HM is shifted to  $CMC_1 = 0.2$   
72 mM. The magnitude of the shift seems to be rather insensitive to the calixarene concentration (at  
73 least from 0.1 to 5 mM). Similarly, below the charge neutralization point, the aggregation  
74 number ( $N$ ) also seems to be fairly independent of the SC6HM and  $C_{12}TAB$  concentrations  
75 ( $N\approx 20-25$ ). For a constant concentration of SC6HM and above the charge neutralization point,  
76  $N$  increases linearly with the concentration of  $C_{12}TAB$ . Despite of this increase, it was also  
77 observed that only a small fraction of added surfactant is absorbed by the micelles and the main  
78 fraction remains free in bulk solution. As a consequence, when the concentration of free  
79 surfactant reaches a value equal to the  $CMC_0$  a second aggregation process is observed ( $CMC_2$ ).

80 In previous work, we were able to estimate the concentration of free  $C_{12}TAB$  and the  
81 micellized  $C_{12}TAB:SC6HM$  ratio above the  $CMC_1$  from self-diffusion coefficients obtained by  
82 DOSY NMR experiments.<sup>12</sup> The results illustrate that the concentration of free  $C_{12}TAB$  is  
83 approximately constant and equal to the  $CMC_1$  for total concentrations of surfactant slightly  
84 below the charge neutralization point. This means that above the  $CMC_1$ , all surfactant molecules  
85 added to the solution are transformed into micelles, as a consequence of the highly cooperative  
86 micellization process. Above the charge neutralization point the concentration of free  $C_{12}TAB$   
87 increase linearly with the total surfactant concentration until a second aggregation process is  
88 observed and a new plateau is reached. This behavior suggests that the aggregation mechanism  
89 switches from cooperative to non-cooperative around the charge neutralization point, switching  
90 again to cooperative above the second aggregation process. The dependence of the *micellized*  
91  $C_{12}TAB:SC6HM$  ratio on the total surfactant concentration also provides important information  
92 for the complete understanding of the system. Within the non-cooperative range there is an

93 increase in this parameter from 4 to 8 suggesting a transition from negatively charged to  
94 positively charged micelles (SC6HM is a hexanion). Above the second aggregation process the  
95 *micellized* C<sub>12</sub>TAB:SC6HM ratio shows a significant increase due to the dilution of the  
96 SC6HM-rich micelles within the new aggregates. While it is not clear if the Br<sup>-</sup> anions  
97 participate in the stabilization of the cationic SC6HM-rich micelles it is obvious that they must  
98 be present in the aggregates formed above the second aggregation process.

99         With the objective of getting further insights into this intriguing and complex behavior  
100 we decided to investigate this system using the hydrolysis of 4-methoxybenzenesulfonyl  
101 chloride (MBSC) and the basic hydrolysis of *p*-nitrophenylvalerate (NPV) as kinetic probes,  
102 together with capillary electrophoresis experiments. Despite being far less popular than  
103 fluorescent or colorimetric probes, reactivity probes provide a powerful methodology to  
104 investigate the aggregation, counterion binding and interfacial properties of self-organized  
105 systems based on amphiphilic compounds.<sup>27-31</sup>

106

## 107 **EXPERIMENTAL SECTION**

108 All chemicals used were of the highest commercially available purity and none required further  
109 purification. Hexamethylated *p*-sulfonatocalix[6]arene was available from previous studies.<sup>9,12,13</sup>  
110 4-Methoxybenzenesulfonyl chloride (MBSC) and *p*-nitrophenylvalerate (NPV) stock solutions  
111 were prepared in acetonitrile, due to their instability in water. The final acetonitrile  
112 concentration in the reaction medium was 1% (v/v).

113         Kinetic runs were initiated by injecting 30 μL of MBSC or NPV stock solution into a 1  
114 cm path length cuvette containing all other compounds dissolved in 2970 μL of water. Reaction  
115 kinetics were recorded by measuring the absorbance changes at 295 nm in the case of MBSC or  
116 at 400 nm for the basic hydrolysis of NPV in a Cary 50 UV-Vis spectrophotometer equipped  
117 with a cell holder thermostated at (25.0±0.1)°C. The MBSC and NPV concentrations were  
118 always 1.0 x 10<sup>-4</sup> M and 2.6 x 10<sup>-5</sup> M, respectively. The absorbance-time data of all kinetic

119 experiments were fitted by first-order integrated equations, and the values of the pseudo-first-  
120 order rate constants ( $k_{\text{obs}}$ ) were reproducible to within 3%.

121 Electrophoretic analysis were made on an Agilent CE<sup>3D</sup> capillary electrophoresis  
122 system, with on-column diode-array detection at  $25 \pm 0.5$  °C and electropherograms were  
123 monitored at 200 nm for SC6HM and 235 nm for thiourea using data treatment software (HP  
124 Chemstation). Fused-silica capillaries (Microtube, Araraquara, Brazil) with total length 48.5  
125 cm, effective length 40.0 cm, and 50  $\mu\text{m}$  i.d. were used in all experiments. The  
126 capillaries were conditioned by flushing with 1 M NaOH (5 min), deionized water (5  
127 min) and electrolyte solution (10 min). Between experiments, the capillary was  
128 reconditioned by flushing 2 min with the background electrolyte (BGE) containing 5  
129 mM sodium tetraborate (TBS), pH = 9.2. In order to evaluate the interaction of C<sub>12</sub>TAB with  
130 SC6HM, the BGE containing 5 mM TBS was enriched with C<sub>12</sub>TAB in concentrations ranging  
131 from 0.04 mM to 50 mM. Samples containing SC6HM 0.5 mM, 140 mg/L of thiourea (fixed;  
132 electroosmotic flow marker) and were diluted with BGE with different contents of C<sub>12</sub>TAB. The  
133 pressure, analysis voltage and time of sample injections were performed in accordance with the  
134 concentration of C<sub>12</sub>TAB: +50 mBar, + 25 kV, 5s for the 0.04 mM to 0.12 mM; -50 mBar, +25  
135 kV, 5s to see the SC6HM and -50 mBar, -25 kV, 5s to see the EOF for the 0.16 mM to 2 mM  
136 concentrations; 2.2mM to 50 mM was used -50 mBar, +25kV, 5s. Electroosmotic mobility was  
137 calculated from the migration time of thiourea (neutral marker). Electropherograms were plotted  
138 in effective mobility scale using the following equation:

$$\mu_{ep} = \frac{L_{eff}}{E} \left( \frac{1}{t_{cal}} - \frac{1}{t_{eof}} \right) \quad (1)$$

139 where  $\mu_{ep}$  is the effective mobility,  $L_{eff}$  is the total capillary length, E the applied electric field,  
140  $t_{cal}$  is the apparent detection time, and  $t_{eof}$  is the detection time of the neutral marker. The  
141 effective mobility was calculated according procedures described previously.<sup>32</sup>

142

143

144 **RESULTS AND DISCUSSION**

145 **Electrophoresis.** The quantification of the concentration of *free* C<sub>12</sub>TAB and of the *micellized*  
146 C<sub>12</sub>TAB:SC6HM ratio from self-diffusion coefficients required approximations regarding the  
147 diffusion coefficients of the aggregates.<sup>12</sup> In order to confirm the previous analysis, the charged  
148 nature of the aggregates was examined using capillary electrophoresis (CE).<sup>32</sup> CE separations  
149 are based on measurements of the difference in mobility of charged compounds (or aggregates)  
150 as a function of applied voltage. Thus, the interaction between SC6HM and C<sub>12</sub>TAB was  
151 examined by CE, using the conditions described in the experimental section and the  
152 experimental results are shown in Figures 1A to 1E.

153 As can be seen in Figure 1A, when the surfactant concentrations are in the range of 0.04  
154 mM to 0.12 mM, the calixarene peak (labeled as 2) shows up after the EOF marker (peak 1).  
155 The results is consistent with expectations, since the CE analysis were performed in the counter  
156 electrosmotic flow mode, and the results are indicating that the SC6HM:C<sub>12</sub>TAB aggregate is  
157 negatively charged. Subsequently, as the concentration of C<sub>12</sub>TAB increases (values in the range  
158 of 0,16 – 2,0mM C<sub>12</sub>TAB, Figures 1B and 1C), shows that additional surfactant monomers are  
159 incorporated into the SC6HM:C<sub>12</sub>TAB aggregate and, as a consequence, there is a considerable  
160 decrease in electrophoretic mobility, which reaches null electrophoretic mobility values with  
161 3mM of C<sub>12</sub>TAB (Figure 1 D). Experiments with surfactant concentration in the range of 3 to  
162 18 mM, when the surfactant is in large excess in relation to the calixarene, the aggregate formed  
163 between surfactant and calixarene is positive charged. Finally, when [C<sub>12</sub>TAB] > CMC,  
164 micelles of C<sub>12</sub>TAB are formed and the SC6HM molecules will be distributed between the  
165 micelles, in a typical cationic aggregate (Figure 1E). The change in electrophoretic mobility as a  
166 function of surfactant concentration can be observed in Figure 2.

167

168

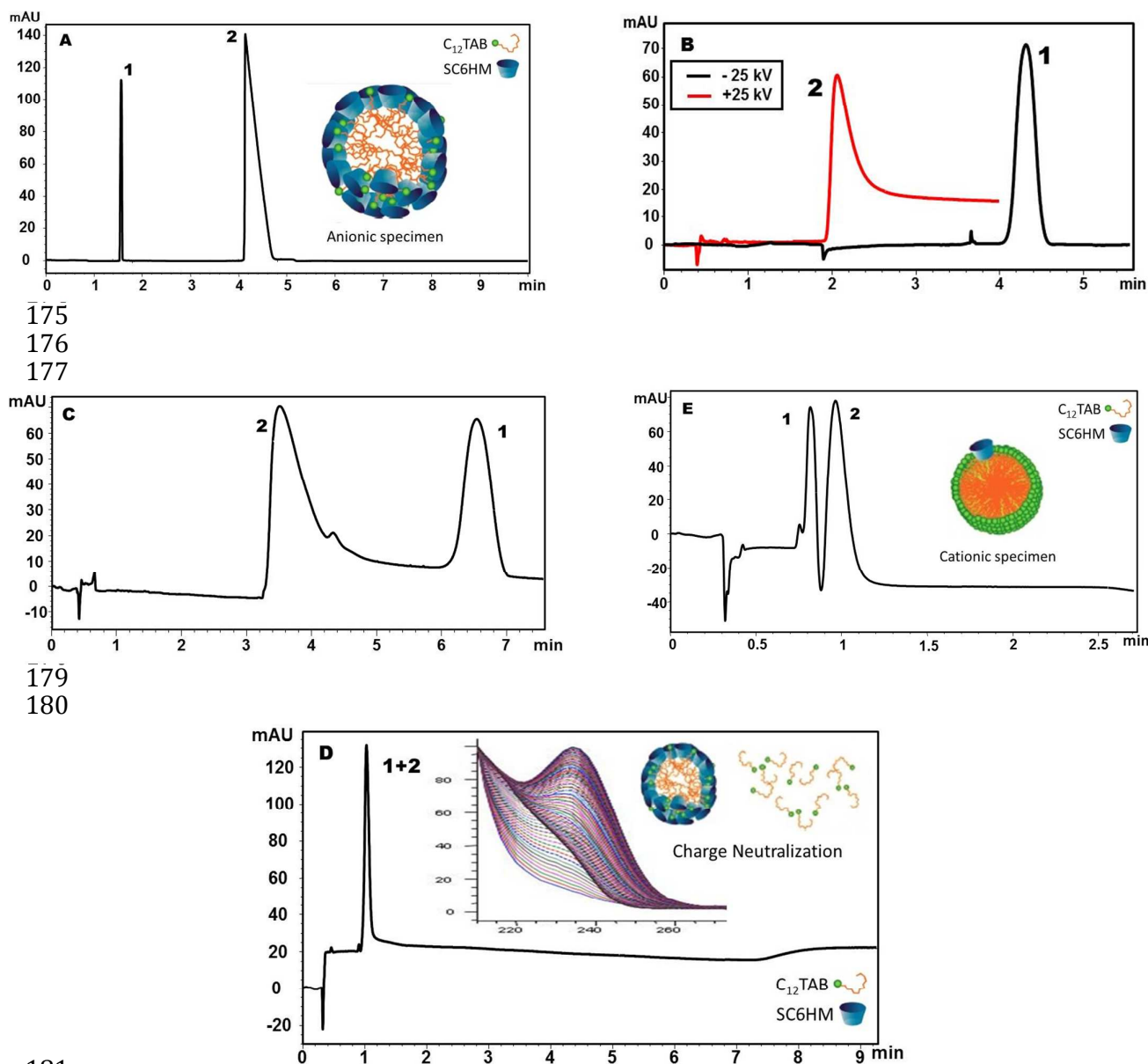
169

170

171

172

173



175

176

177

179

180

181

182

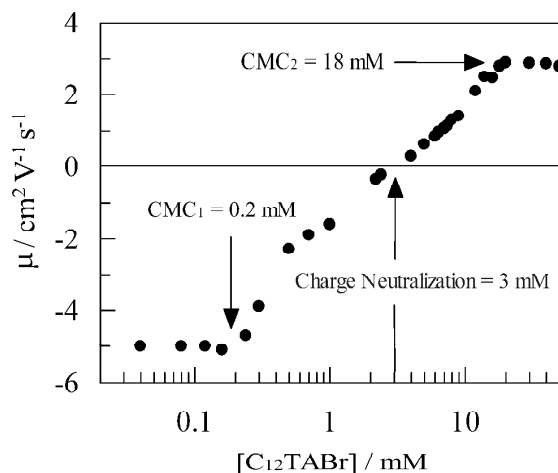
183 **Figure 1.**(A) Electropherogram profile of concentration of C<sub>12</sub>TAB varying from 0.04 mM to 0.12 mM  
 184 (+50 mBar, +25 kV, 5 s); (B) 0.16 mM to 2.0 mM (-50 mBar, +25 kV, 5 s to SC6HM and -50 mBar, -25 kV,  
 185 5 s to EOF); (C) 2.2 mM – 2.8 mM (-50 mBar, +25 kV, 5 s); (D) EOF + SC6HM (neutral) at ~3 mM (-50  
 186 mBar, +25 kV, 5 s); (E) electropherogram > 3.4 mM to 50 mM of C<sub>12</sub>TAB (-50 mBar, +25 kV, 5 s). 1-EOF; 2-  
 187 SC6HM;

188

189

190 The analysis of the mobility of the calixarene as a function of the concentration of C<sub>12</sub>TAB  
 191 shown in Figure 2, allows observing several critical points. The first one is around 0.2 mM, and  
 192 indicates the onset of the incorporation of surfactant molecules into the calixarenes and is  
 193 denominated as (CMC<sub>1</sub>), where the anionic species is predominant. After this point the  
 194 electrophoretic mobility increases, crossing the null electrophoretic mobility value around  
 195 3mM, which corresponds to a 6:1 ratio of C<sub>12</sub>TAB molecules for each SC6HM, in good  
 196 agreement with previous conclusions based on NMR data. Increasing the concentration of  
 197 surfactant above 3.0 mM, the SC6HM:C<sub>12</sub>TAB aggregates become positively charged. These  
 198 values are consistent with those reported in a previous study performed using conductivity  
 199 analysis.<sup>12</sup> The third inflexion point, at 18mM, indicates CMC<sub>2</sub> of free surfactant in good  
 200 agreement with that previously obtained by conductivity.<sup>12</sup> Overall, the results described here  
 201 provide direct evidence for the transformation of anionic into cationic micelles in this system.

202



203  
 204  
 205  
 206  
 207

**Figure 2.** Dependence of the electrophoretic mobility data with the concentration of C<sub>12</sub>TAB in the presence of 0.5 mM of SC6HM.

208 The changes in electrophoretic mobility, shown in Figure 2, can be conveniently used to  
 209 estimate zeta potentials ( $\zeta_m$ ) by means of equation 2, which relates the charge of the micelle to  
 210 its mobility:

$$\zeta_m = \frac{\mu \eta}{\varepsilon_0 \varepsilon f(\kappa R_m)} \quad (2)$$

211 where  $\eta$  is the viscosity of the medium,  $f(\kappa R_m)$  corresponds to Henry's function,  $\kappa$  is the  
212 Debye-Hückel shielding parameter ( $\text{m}^{-1}$ ),  $R_m$  is the radius of  $\text{C}_{12}\text{TAB}$  micelle, and  $\epsilon_0$  and  $\epsilon$   
213 correspond to the vacuum permittivity and the relative permittivity of the solvent.<sup>33,34</sup>

214 Initially, the zeta potential of the  $\text{C}_{12}\text{TAB}$  micelle was calculated above the  $\text{CMC}_2$  of free  
215 surfactant, where the behavior should be closely related to a solution of  $\text{C}_{12}\text{TAB}$  without  
216 additives. In order to proceed with the calculation of Zeta potential, we adopted the reported  
217 radii values ( $R_m$ ) of the  $\text{C}_{12}\text{TAB}$  micelle of 20 Å.<sup>35</sup> Considering the ionic strength of the  
218 supporting electrolyte (TBS = 0.005 M), it is possible to estimate a value of  $\kappa = 2.3 \times 10^8 \text{ m}^{-1}$ ,  
219 and accordingly, under our experimental conditions  $\kappa R_m$  for  $\text{C}_{12}\text{TAB}$  micelles is 0.46, which  
220 allowed us to calculate the value of Henry's function  $f(\kappa R_m) = 0.69$ , following Ohshima's  
221 approximation.<sup>34</sup>

222 Using the value of Henry's function was possible to estimate the zeta potentials of the  
223 aggregates, and as shown in Table 1, the Zeta potential ( $\zeta_m$ , in mV) above  $\text{CMC}_2$  is 50.4  
224 millivolts, a value which is consistent with those reported in the literature for  $\text{C}_{12}\text{TAB}$  micelles.  
225 The mobility of the SC6HM anionic calixarene, for  $[\text{C}_{12}\text{TAB}] \leq \text{CMC}_1$  is constant and probably  
226 reflects the mobility of the individual SC6HM molecules or of small aggregates. A crucial point  
227 is the behavior at  $\text{CMC}_1$  (~0.2 mM), which corresponds to the formation of anionic aggregates  
228 of the calixarenes supramolecularly complexed with  $\text{C}_{12}\text{TAB}$  and we could calculate a zeta  
229 potential of -47.2 millivolts, using a micellar radius of 20 Å and the same approximations  
230 described above to calculate Henry's function. Between  $\text{CMC}_1$  and  $\text{CMC}_2$  the change in Zeta  
231 potential follows linearly the changes in mobility and, it is interesting to observe that the charge  
232 neutrality of the aggregate is attained when the  $[\text{C}_{12}\text{TAB}] = 3.0 \text{ mM}$ , which corresponds exactly  
233 to a ratio of ( $[\text{surfactant}]/[\text{calixarene}]$ ) = 6, which is the theoretically expected neutralization  
234 point for an optimum effect of the complexation. Above a ratio of 6 surfactant molecules for  
235 each calixarene, the aggregate becomes increasingly positively charged, finally reaching zeta  
236 potential values which are closely similar to that of a pure  $\text{C}_{12}\text{TAB}$  cationic micelle.<sup>35</sup>

237

238

239

240

241

**Table 1.** Zeta potential values for each different aggregate formed.<sup>a</sup>

Point	Charge of Aggregate	Concentration (mM)	$\zeta_m$ (mV)
CMC <sub>2</sub>	Cationic Micelle	18.0	50.40
Neutral point	Neutral point	3.0	0
CMC <sub>1</sub>	Anionic Micelle	0.2	-47.15

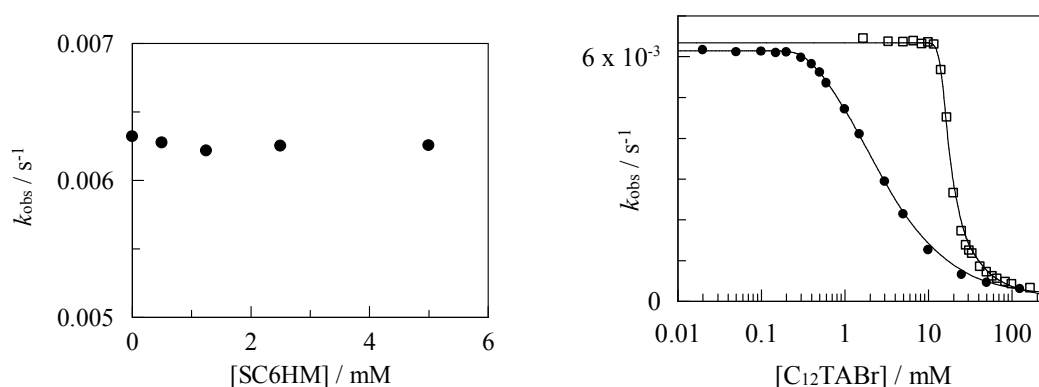
242 <sup>a</sup>[SC6HM] = 0.5 mM,  $T = 25^\circ\text{C}$ .

243

244 **Hydrolysis of MBSC.** Another important feature to be investigated in the present system is the  
 245 capacity of these supramolecular micelles to solubilize guest molecules or ions and test their  
 246 potential to be used as nanoreactors. Using simple reactions as kinetic probes will allow these  
 247 parameters to be investigated as well the micellar polarity and effect of the micellar charge on  
 248 the compartmentalization of the reactants.

249 The rate of the solvolysis of MBSC is highly sensitive to the polarity of the  
 250 (micro)environment in which the probe is located. Therefore this reaction has been recurrently  
 251 used as a probe to investigate micellar and host-guest systems.<sup>30,36</sup> In general, the reaction rate  
 252 decreases as the probe is transferred from bulk water to more apolar medium such as the  
 253 micellar interior/interface or the cavity of a macrocyclic container. The results depicted in  
 254 Figure 3-left suggest that MBSC does not interact with SC6HM in this concentration range, or  
 255 that the observed rate constant for the solvolysis does not vary significantly from the bulk to the  
 256 SC6HM pseudo-cavity: or both. SC6HM is highly flexible and is believed to exist in solution as  
 257 a mixture of several interconverting conformers, thus lacking a defined structure/cavity.<sup>37,38</sup> As a  
 258 result of this poorly defined geometry, SC6HM usually displays weaker binding abilities  
 259 comparatively to more pre organized derivatives. The instability of MSBC in aqueous solution

260 precludes the utilization of more conventional techniques to confirm or rule out the  
 261 complexation of MSBC with SC6HM.



262

263

264 **Figure 3.(Left)** Influence of the SC6HM on the observed rate constant ( $k_{\text{obs}}$ ) for the hydrolysis of MBSC.  
 265 **(Right)** Variation of  $k_{\text{obs}}$  with  $[\text{C}_{12}\text{TABr}]$  in the absence (open squares) and in the presence of 5 mM of  
 266 SC6HM (filled circles). All kinetic experiments were conducted at 25 °C in water with 1% acetonitrile  
 267 (v/v).  
 268

269

270 Figure 3-right shows the changes observed for  $k_{\text{obs}}$  as a function of the  $\text{C}_{12}\text{TABr}$   
 271 concentration in the absence and presence of 5 mM of SC6HM. The plot can be divided into  
 272 two regions: a first one that corresponds to low surfactant concentration where the rate of the  
 273 hydrolysis of MBSC is essentially constant and a second one above a certain critical  
 274 concentration, that is identified by the point at which the  $k_{\text{obs}}$  starts decreasing. This point is  
 275 identified as the onset of micelle formation (the critical micelle concentration, CMC) and the  
 276 decrease observed for  $k_{\text{obs}}$  is attributed to the incorporation of MBSC within the micellar  
 277 aggregates, a lower polarity microenvironment that inhibits the hydrolysis of the probe. The  
 278  $\text{CMC}_0$  and  $\text{CMC}_1$  values obtained from the kinetic data, 13mM and 0.25 mM in the absence and  
 279 presence of 5 mM of SC6HM, respectively, are in good agreement with those previously  
 280 obtained by other techniques.<sup>12,13</sup>

281 The kinetic data can be quantitatively analyzed through the application of the  
 282 pseudophase formalism. This simple theory considers that molecules and ions present in  
 283 solutions are distributed between two well-differentiated environments: bulk water and a

284 micellar pseudophase. For reactions taking place in the sub-second and slower timescales the  
 285 partition of the reactants between the bulk and the micellar pseudophase can be considered as a  
 286 fast equilibrium so that the observed rate constant is given by the molar fraction weighted  
 287 average of the rate constants corresponding to the reaction taking place in the two environments.

288 As shown elsewhere,  $k_{obs}$  is given by equation 3.<sup>39</sup>

289

$$k_{obs} = \frac{k_w + k_m K_S^m [D_n]}{1 + K_S^m [D_n]} \quad (3)$$

290

291 Where  $k_w$  is the rate constant for the hydrolysis reaction taking place in bulk water,  $k_m$  is the rate  
 292 constant for the reaction taking place in the micellar pseudophase,  $K_S^m$  is the binding constant of  
 293 MBSC between the bulk and the micelles (defined as  $K_S^m = [MBSC]_m / [MBSC]_w [D_n]$ ) and  
 294  $[D_n]$  is the concentration of micellized surfactant that can be approximated as  $[D_n] =$   
 295  $[\text{surfactant}]_0 - \text{CMC}$ ; where  $[\text{surfactant}]_0$  is the total concentration of surfactant. At this point it  
 296 must be stressed that the approximation used to obtain  $[D_n]$  does not apply for low  
 297 concentrations of SC6HM because after neutralization of the calixarene charge, the  
 298 concentration of free surfactant increases significantly before a second aggregation process take  
 299 place.<sup>12</sup> Nevertheless, for concentrations of SC6HM with charge neutralization point well above  
 300 the  $\text{CMC}_0$  of pure surfactant (14 mM), this behavior is not observed, or insignificant.<sup>13</sup> In the  
 301 present work the concentration of SC6HM (5 mM) corresponds to a charge neutralization point  
 302 of 30 mM, well above the  $\text{CMC}_0$ .

303 As can be observed in Figure 3-right, the  $k_{obs}$  data is satisfactorily fitted by equation 3.

304 Fitting was achieved with  $k_w = (6.3 \pm 0.1) \times 10^{-3} \text{ s}^{-1}$ ,  $k_m = (1.6 \pm 0.4) \times 10^{-4} \text{ s}^{-1}$  and  $K_S^m =$   
 305  $(2.7 \pm 0.2) \times 10^2 \text{ M}^{-1}$  in the absence of SC6HM and  $k_w = (6.1 \pm 0.1) \times 10^{-3} \text{ s}^{-1}$ ,  $k_m = (1.7 \pm 0.2) \times 10^{-4} \text{ s}^{-1}$   
 306 and  $K_S^m = (4.3 \pm 0.1) \times 10^2 \text{ M}^{-1}$  in the presence of 5 mM of SC6HM. The results obtained in the  
 307 absence of SC6HM are in good agreement with those reported in the literature.<sup>30</sup> When both sets  
 308 of results are compared it can be seen that  $k_m$  has the same value in the absence and in the  
 309 presence of calixarene. However it was shown previously that, in the case of MBSC, this

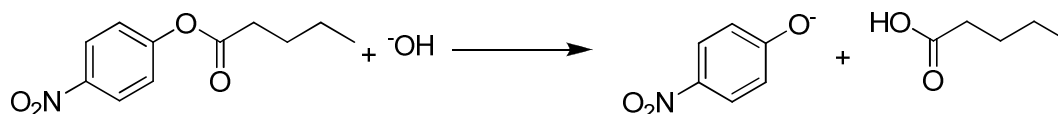
310 parameter does not indicate a significant dependence on the hydrophobic character or the  
311 interfacial charge and polarity of the micellar aggregates.<sup>30,40</sup> On the other hand, the  $K_S^m$  value  
312 shows a significant increase in the presence of SC6HM suggesting that the mixed micelles are  
313 more hydrophobic than pure aggregates, with the absolute value being close to that observed for  
314 C<sub>16</sub>TAC ( $K_S^m = [4.7 \pm 0.3] \times 10^2 \text{ M}^{-1}$ ).<sup>30</sup>

315

316 **Basic hydrolysis of NPV.** Because the hydrolysis of MBSC does not provide significant  
317 information on the interfacial properties of the micellar aggregates, another probe reaction was  
318 used to investigate it. Bimolecular reactions of hydrophobic organic compounds and ionic  
319 reactants are very convenient probes to get insights into the ionic composition of micellar  
320 interfaces.<sup>27</sup> The basic hydrolysis of nitrophenyl esters has become an iconic reaction in studies  
321 concerning self-assembled amphiphilic systems based on cationic surfactants. In this work the  
322 basic hydrolysis of *p*-nitrophenylvalerate was selected as a probe reaction (SCHEME 1) to  
323 investigate the ionic composition of micellar aggregates formed from SC6HM:C<sub>12</sub>TAB  
324 supramphiphile.

325

326



327

328

SCHEME 1. Basic hydrolysis of *p*-nitrophenylvalerate.

329

330

331 As a basis for the study of the basic hydrolysis of *p*-nitrophenylvalerate (NPV) in the  
332 complex system formed by SC6HM and C<sub>12</sub>TAB, the influence of each component was  
333 investigated separately. Figure 4-left shows the changes observed on the rate of the reaction in  
334 the presence of increasing concentration of SC6HM. The results suggest that NPV forms a  
335 complex with SC6HM (with  $K = 13 \pm 6 \text{ M}^{-1}$  obtained from the non-linear data fit assuming a 1:1

336 complex) which stabilizes the guest in basic conditions ( $k_{\text{obs}}$  decreases) probably due to  
 337 repulsion of  $\text{OH}^-$  ions by the sulfonate groups of the host. Nevertheless, the association constant  
 338 is very low, probably due to the lack of preorganization of the receptor, and for 5 mM of  
 339 SC6HM the fraction of complexed NPV is very low (ca. 6%).

340

341

342

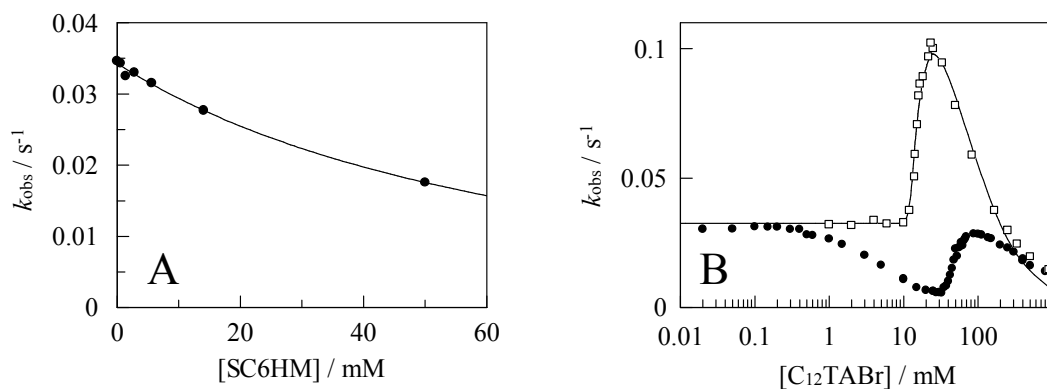
343

344

345

346

347



348

349

350 **Figure 4.**(Left) Influence of the SC6HM on the observed rate constant ( $k_{\text{obs}}$ ) for the basic  
 351 hydrolysis of NPV. (Right) Variation of  $k_{\text{obs}}$  with  $[\text{C}_{12}\text{TABr}]$  in the absence (open squares)  
 352 and in the presence of 5 mM of SC6HM (filled circles). All kinetic experiments were  
 353 conducted at 25 °C in water with  $[\text{NaOH}] = 5 \text{ mM}$  and 1% acetonitrile (v/v).

353

354

355

356

357

358

359

360

361

362

363

364

Figure 4-right shows the dependence of  $k_{\text{obs}}$  with the concentration of  $\text{C}_{12}\text{TABr}$  in the  
 absence of SC6HM (open squares). The data follow the expected trend for bimolecular reactions  
 of organic compounds with anionic reactants in the presence of cationic micelles.<sup>27</sup> The  $k_{\text{obs}}$  is  
 constant for concentrations of surfactant below the  $\text{CMC}_0$  (12 mM). It worth noting that this  
 value is slightly below that determined above due to the higher salt concentration (NaOH).  
 Above this point the apparent reaction rate increases due to the incorporation of NPV and  $\text{OH}^-$   
 in the micellar surface, increasing the local concentrations of both reactants. The reaction rate  
 reaches a maximum value and then decreases for higher concentration of surfactant. This  
 behavior is attributed to the competitive binding of inert  $\text{Br}^-$  anions that displace reactive  $\text{OH}^-$   
 anions to the bulk aqueous solution.

365 The results depicted in Figure 4-right can be quantitatively analyzed through the  
 366 application of the pseudophase ion exchange model (equations 4 and 5).<sup>27</sup>In equations 4 and 5  
 367  $k_m$ ,  $K_s^m$  and  $[D_n]$  are the same as in equation 3 while  $m_{OH}$ ,  $\beta$  and  $K_{OH}^{Br}$  are the concentration of  
 368  $^-OH$  ions in the micellar pseudophase (defined as the mole ratio  $[^-OH]/[D_n]$ ), the degree of  
 369 counterion binding (which is assumed to be constant) and the ionic exchange equilibrium  
 370 constant ( $K_{OH}^{Br} = [OH]_w[Br]_M/[OH]_M[Br]_w$ ), respectively. By computing the values of  $m_{OH}$   
 371 from equation 5, using previously determined values for  $\beta = 0.8$  and  $K_{OH}^{Br} = 17$ , equation 4 can be  
 372 used to fit the  $k_{obs}$  data represented in figure 4-right. As can be observed the theoretical curve  
 373 fits reasonably well the experimental data for concentrations of surfactant below ca. 200 mM  
 374 but for higher concentration it starts to deviate from the data points. This behavior is well  
 375 documented and is related to the known limitations of the pseudophase ion exchange model for  
 376 high concentrations of surfactant.<sup>27,39</sup> From the fitting procedure the following values were  
 377 obtained:  $k_w = 6.5 \pm 0.1 \text{ M}^{-1} \text{ s}^{-1}$ ,  $K_s^m = (1.4 \pm 0.2) \times 10^2 \text{ M}^{-1}$  and  $k_m = 8.5 \pm 0.9 \text{ s}^{-1}$ .  $k_m$  is an  
 378 apparent rate constant that is related to the bimolecular rate constant ( $k'_m$ ) for basic hydrolysis  
 379 of the NPV located within the micellar aggregates through the relation  $k_m = k'_m / V_m$ , where  $V_m$   
 380 is the molar volume of the Stern layer ( $0.14 \text{ M}^{-1}$ ).<sup>41-43</sup> From this relation,  $k'_m = 1.2 \text{ M}^{-1} \text{ s}^{-1}$  can be  
 381 obtained. When compared with  $k_w$  it is clear that the observed rate enhancement is due to an  
 382 increase in the local concentrations of the reactants rather than to a true catalytic effect.

383

$$k_{obs} = \left( \frac{k_w[HO^-]_0 + (k_m K_s^m - k_w)m_{OH}[D_n]}{1 + K_s^m[D_n]} \right) \quad (4)$$

384

$$m_{OH}^2 + \left\{ \frac{(K_{OH}^{Br}[Br^-]_0 + [HO^-]_0)}{(K_{OH}^{Br} - 1)[D_n]} - \beta \right\} m_{OH} - \frac{\beta[HO^-]_0}{(K_{OH}^{Br} - 1)[D_n]} = 0 \quad (5)$$

385

386 In the presence of 5 mM of SC6HM (figure 4-right, closed circles), the  $k_{obs}$  values  
 387 follow a different trend from that observed in the absence of calixarene. At 0.2 mM ( $CMC_1$ ) the  
 388 apparent rate constant starts dropping due to the incorporation of NPV into the mixed

389 SC6HM:C12TAB micelles that form above this concentration. Drawing a parallel with the  
390 behavior observed in the absence of SC6HM, the observed decrease in  $k_{\text{obs}}$  suggests that the  
391 micellar aggregates formed in the concentration range between 0.2 and 30 mM do not contain  
392 exchangeable  $\text{Br}^-/\text{OH}^-$  counterions because in this case a change in  $k_{\text{obs}}$  should be observed. This  
393 means that within this concentration range the micelles are exclusively formed by SC6HM and  
394  $\text{C}_{12}\text{TAB}$ . Above 30 mM the  $k_{\text{obs}}$  values display a sharp increase, reach a maximum value and  
395 drop again. Further, for high concentrations of  $\text{C}_{12}\text{TAB}$  the kinetic data attain the values  
396 obtained in the absence of SC6HM. This behavior is typical of cationic micelles with  
397 exchangeable counterions and indicates that the mixed micelles are gradually transformed into  
398 “quasi like” micelles as the concentration of SC6HM becomes more diluted within the  
399 aggregates.

400

401

## 402 CONCLUSIONS

403 This work demonstrates that supra-amphiphiles formed from SC6HM and  $\text{C}_{12}\text{TAB}$  aggregate  
404 into micellar aggregates with tunable degrees of ionization. For low  $\text{C}_{12}\text{TAB}:\text{SC6HM}$  molar  
405 ratios the micelles are negatively charged. As the concentration of  $\text{C}_{12}\text{TAB}$  increases the  
406 negative micellar charge decreases and reaches neutrality at  $\text{C}_{12}\text{TAB}:\text{SC6HM} \approx 6$ . Above this  
407 point the micelles become positively charged and their ability to solubilize more  $\text{C}_{12}\text{TAB}$   
408 decreases substantially. As a result the fraction of free  $\text{C}_{12}\text{TAB}$  also increases until it reaches a  
409 new critical concentration leading to a second aggregation process.

410 The kinetics of the MBSC hydrolysis and NPV basic hydrolysis show that  $\text{C}_{12}\text{TAB}:\text{SC6HM}$   
411 micelles have the ability to solubilize hydrophobic compounds within their structure. This result  
412 together with their reduced CMC demonstrate the higher potential of  $\text{C}_{12}\text{TAB}:\text{SC6HM}$  based  
413 supramphiphiles compared with conventional surfactants. The basic hydrolysis of NPV was  
414 shown to be a very effective probe to investigate the ionic composition of the micellar interface  
415 in this complex system. The results suggest that  $\text{Br}^-$  do not participate in the micelles formed  
416 between the first and second CMC's. Above this last point, the micellized  $\text{C}_{12}\text{TAB}:\text{SC6HM}$

417 ratio increases significantly and the counteranions are transferred into the micellar interface  
418 screening the electrostatic repulsion between positively charged C<sub>12</sub>TAB molecules.

419

#### 420 **ACKNOWLEDGEMENTS**

421 N.B. acknowledges the Fundação para a Ciência e Tecnologia (FCT, Portugal) for a postdoctoral  
422 grant (SFRH/BPD/84805/2012). We are grateful to INCT-Catálise/ CNPq, PRONEX, FAPESC,  
423 CSF/CNPq and CAPES for their support of this work. We acknowledge financial support from  
424 the Ministerio de Economía y Competitividad of Spain (project CTQ2011-22436) and Xunta de  
425 Galicia (2007/085).

426

## 427 REFERENCES

- 428 (1) M. J. Rosen, *Surfactants and Interfacial Phenomena*, 3rd ed.; John Wiley & Sons  
429 Ltd: Hoboken, NJ, 2004.
- 430 (2) K. Holmberg, B. Jönsson, B. Kronberg, B. Lindman, *Surfactants and Polymers in*  
431 *Aqueous Solution*, 3rd ed., John Wiley & Sons Ltd: Chichester, UK, 2002.
- 432 (3) F. M. Menger, L. Shi, S. A. A. Rizvi, *J. Am. Chem. Soc.*, 2009, **131**, 10380–  
433 10381.
- 434 (4) F. M. Menger, S. A. A. Rizvi, *Langmuir*, 2011, **27**, 13975–13977.
- 435 (5) F. A. García Daza, A. D. Mackie, *J. Phys. Chem. Lett.*, 2014, **5**, 2027–2032.
- 436 (6) Y. Kang, K. Liu, X. Zhang, *Langmuir*, 2014, **30**, 5989–6001.
- 437 (7) X. Zhang, C. Wang, *Chem. Soc. Rev.*, 2011, **40**, 94–101.
- 438 (8) C. Wang, Z. Wang, X. Zhang, *Acc. Chem. Res.*, 2012, **45**, 608–618.
- 439 (9) N. Basilio, M. Martín-Pastor, L. García-Río, *Langmuir*, 2012, **28**, 6561–6568.
- 440 (10) N. Basilio, V. Francisco, L. Garcia-Rio, *Int. J. Mol. Sci.*, 2013, **14**, 3140–3157.
- 441 (11) V. Francisco, N. Basilio, L. Garcia-Rio, J. R. Leis, E. F. Marques, C. Vázquez-  
442 Vázquez, *Chem. Commun.*, 2010, **46**, 6551–6553.
- 443 (12) N. Basilio, B. Gómez, L. Garcia-Rio, V. Francisco, *Chem. -Eur. J.*, 2013, **19**,  
444 4570–4576.
- 445 (13) N. Basilio, L. García-Río, *Chem. -Eur. J.*, 2009, **15**, 9315–9319.
- 446 (14) D.-S. Guo, Y. Liu, *Acc. Chem. Res.*, 2014, **47**, 1925–1934.
- 447 (15) B.-P. Jiang, D.-S. Guo, Y.-C. Liu, K.-P. Wang, Y. Liu, *ACS Nano*, 2014, **8**,  
448 1609–1618.
- 449 (16) Z. Qin, D.-S. Guo, X.-N. Gao, Y. Liu, *Soft Matter*, 2014, **10**, 2253–2263.
- 450 (17) K. Wang, D.-S. Guo, M.-Y. Zhao, Y. Liu, *Chem. -Eur. J.*, 2014, DOI:  
451 10.1002/chem.201303963.
- 452 (18) Y. Cao, Y. Wang, D. Guo, Y. Liu, *Sci. China Chem.*, 2013, **57**, 371–378.
- 453 (19) D.-S. Guo, B.-P. Jiang, X. Wang, Y. Liu, *Org. Biomol. Chem.*, 2012, **10**, 720–  
454 723.

- 455 (20) D.-S. Guo, K. Wang, Y.-X. Wang, Y. Liu, *J. Am. Chem. Soc.*, 2012, **134**, 10244–  
456 10250.
- 457 (21) Z. Li, C. Hu, Y. Cheng, H. Xu, X. Cao, X. Song, H. Zhang, Y. Liu, *Sci. China*  
458 *Chem.*, 2012, **55**, 2063–2068.
- 459 (22) K. Wang, D. Guo, Y. Liu, *Chem. -Eur. J.*, 2012, **18**, 8758–8764.
- 460 (23) K. Wang, D.-S. Guo, X. Wang, Y. Liu, *ACS Nano*, 2011, **5**, 2880–2894.
- 461 (24) K. Wang, D.-S. Guo, Y. Liu, *Chem. -Eur. J.*, 2010, **16**, 8006–8011.
- 462 (25) V. Wintgens, C. Le Coeur, C. Amiel, J.-M. Guigner, J. G. Harangozó, Z.  
463 Miskolczy, L. Biczók, *Langmuir*, 2013, **29**, 7682–7688.
- 464 (26) G. Gattuso, A. Notti, A. Pappalardo, S. Pappalardo, M. F. Parisi, F. Puntoriero,  
465 *Tetrahedron Lett.*, 2013, **54**, 188–191.
- 466 (27) C. A. Bunton, F. Nome, F. H. Quina, L. S. Romsted, *Acc. Chem. Res.*, 1991, **24**,  
467 357–364.
- 468 (28) Y. Geng, L. S. Romsted, F. Menger, *J. Am. Chem. Soc.*, 2006, **128**, 492–501.
- 469 (29) L. S. Romsted, *Langmuir*, 2007, **23**, 414–424.
- 470 (30) M. Cepeda, R. Daviña, L. García-Río, M. Parajó, P. Rodríguez-Dafonte, M.  
471 Pessêgo, *Org. Biomol. Chem.*, 2013, **11**, 1093–1102.
- 472 (31) J. P. Priebe, F. D. Souza, M. Silva, D. W. Tondo, J. M. Priebe, G. A. Micke, A.  
473 C. O. Costa, C. A. Bunton, F. H. Quina, H. D. Fiedler, F. Nome, *Langmuir*, 2012,  
474 **28**, 1758–1764.
- 475 (32) L. Marte, R. C. Beber, M. A. Farrukh, G. A. Micke, A. C. O. Costa, N. D. Gillitt,  
476 C. A. Bunton, P. Di Profio, G. Savelli, F. Nome, *J. Phys. Chem. B*, 2007, **111**,  
477 9762–9769.
- 478 (33) M. A. Farrukh, R. C. Beber, J. P. Priebe, M. L. Satnami, G. A. Micke, A. C. O.  
479 Costa, H. D. Fiedler, C. A. Bunton, F. Nome, *Langmuir*, 2008, **24**, 12995–13000.
- 480 (34) H. Ohshima, *J. Coll. Interface Sci.*, 1994, **168**, 269–271.
- 481 (35) A. Shukla, H. Rehage, *Langmuir*, 2008, **24**, 8507–8513.
- 482 (36) M. Pessêgo, N. Basilio, J. A. Moreira, L. García-Río, *ChemPhysChem*, 2011, **12**,  
483 1342–1350.
- 484 (37) J. Alvarez, Y. Wang, M. Gómez-Kaifer, A. E. Kaifer, *Chem. Commun.*, 1998,  
485 1455–1456.

- 486 (38) R. Castro, L. A. Godínez, C. M. Criss, A. E. Kaifer, *J. Org. Chem.*, 1997, **62**,  
487 4928–4935.
- 488 (39) C. A. Bunton, L. H. Gan, J. R. Moffatt, L. S. Romsted, G. Savelli, *J. Phys.*  
489 *Chem.*, 1981, **85**, 4118–4125.
- 490 (40) C. A. Bunton, *J. Phys. Org. Chem.*, 2005, **18**, 115–120.
- 491 (41) N. S. Yusof, M. N. Khan, *J. Phys. Chem. B*, 2012, **116**, 2065-2074.
- 492 (42) L. Onel, N. J. Buurma, *J. Phys. Chem. B*, 2011, **115**, 13199-13211.
- 493 (43) M. N. Khan, *Adv. Coll. Interface Sci.*, 2010, **159**, 160-179.
- 494
- 495

496

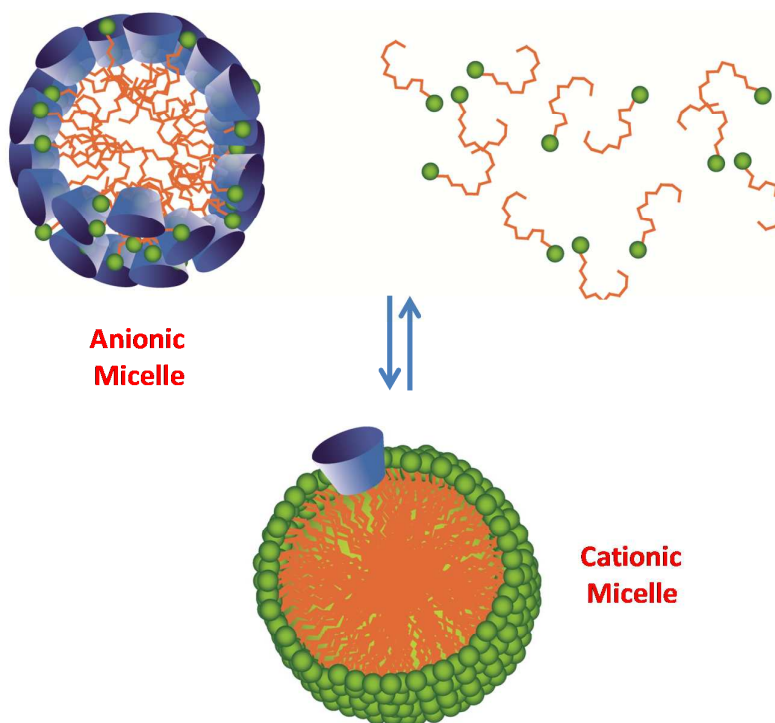
497

498

499

500

## GRAPHICAL ABSTRACT



501